DOI 10.31489/2023No2/20-31
UDC 535.37

EXTRAORDINARY MAGNETORESISTANCE OF LASER ANNEALED NANO BORON DEPOSITED ON OXIDIZED POROUS SILICON

Narjis Zamil Abdulzahra

Department of Physics, College of Science, Al-Nahrain University, Jadriya, Baghdad, Iraq,
ner_ner2@yahoo.com

This study explores the impact of laser annealing on the electrical and magnetic properties of nano boron deposited on oxidized porous silicon (n-B/PSiO$_2$) and its potential for spintronic applications. The Nd: YAG laser was used at varying energies to anneal the n-B thin films. Increasing the laser energy increased grain size and more ordered grain structures. It also increased surface roughness due to forming new grain boundaries and secondary phases. The electrical properties of the material were also affected by the laser annealing, with an increase in forward and reverse current and an increase in electrical resistivity with increased annealing temperature. The study also found that the magnetoresistance of the material increased with increasing laser temperature, attributed to tunnel injection through the thin silicon dioxide layer, and could be up to 7 times higher than non-annealed n-B/PSiO$_2$ in a magnetic field. The study highlights the importance of controlling materials' grain size and structure for their physical and electrical properties. In addition, it provides insights into the electronic properties of n-B/PSiO$_2$ and the behavior of charge carriers in a magnetic field.

Keywords: Extraordinary Magnetoresistance, Laser Annealing, Nano Boron/ Oxidized Porous Silicon, Electrical Properties, Magnetic Properties, Spintronic Applications.

Introduction

Silicon is a material with exceptional promise for magneto electronics, thanks to its long spin coherence of up to 7 meters. However, in conventional micro- and Nanoelectronics, the functional state of a device is determined by electric current and electric field, which can lead to energy dissipation and leakage. Spintronic offers the solution to limitations by manipulating the spin degree of freedom instead of electric current [1]. The demand for non-volatile memories with high storage density, operation speed, and low power consumption has increased in recent years. One promising solution is Resistive Random-Access Memory (RRAM), which has the advantages of high integration, low power consumption, high read-write speed, and compatibility with CMOS technology. RRAM devices are resistors whose electrical resistance can be changed by an externally applied magnetic field. They operate based on the electrodynamics principle of /FB/=q/V//B/sin θ, where the resistance of material's resistance. The material is proportional to the magnetic field [2].

The Extraordinary Magneto Resistance (EMR) effect, discovered in 2000, is more effective than the Giant Magneto Resistance (GMR) effect. When a transverse magnetic field is applied, the EMR effect occurs in semiconductor-metal hybrid systems. At room temperature, it shows lower resistance in the absence of a magnetic field, and when a strong magnetic field has higher resistance, which can operate without physical contact, have many applications, including in MRAM, hard disc drives, magnetometers, ferrous detection, electronic compasses, bio-sensors, position sensors, magnetic field sensors, and for measuring electric current [3]. The conventional theory of magnetoresistance in metals and semiconductors relies on a distribution of scattering times among conducting carriers that a unique Hall field cannot compensate for. According to scientific research, materials with a fast, free electron Fermi surface and a significant charge carrier led to positive magnetoresistance that is quadratic in weak and saturates in strong magnetic fields [4].

Laser annealing is a technique used to modify the properties of a material's surface by applying intense laser pulses. While it is true that the effect of laser annealing on morphological features of the surface is an important aspect to consider, it is essential to note that the specific details regarding these effects may vary depending on the material being annealed and the parameters of the laser annealing process. The general overview of the potential effects of laser annealing on surface morphology is given by[5]; Surface Melting and Solidification: Laser annealing can induce localized melting of the surface material, followed by rapid

solidification as the laser beam moves away. This process can lead to changes in the surface topography, such as the formation of re-solidified regions, which may exhibit different morphological features compared to the original surface; Surface Roughness Modification: Laser annealing can also influence the surface roughness of a material. The energy delivered by the laser can cause material ablation, vaporization, or rearrangement, leading to the smoothing or roughening of the surface [6]. The laser energy density, pulse duration, and repetition rate are crucial parameters that determine the extent of roughness modification; Surface Crystallization: In some cases, laser annealing can induce the recrystallization of the material's surface occurs when the laser energy is sufficient to heat the material above its recrystallization temperature, allowing the atoms or molecules to rearrange into a more ordered crystal structure. This recrystallization process can result in changes in surface grain size, orientation, or texture; Surface Morphological Defects: Depending on the energy and intensity of the laser, certain morphological defects may arise on the material surface. For instance, laser-induced surface ablation can generate pits, craters, or microscale roughness. These defects may affect the material's surface properties and functionality [7].

It is important to note that the specific morphological changes induced by laser annealing will depend on the material properties, laser parameters (such as energy density, pulse duration, and repetition rate), and the desired outcome. Therefore, it is recommended that the authors provide detailed information on the material, laser parameters, and characterization techniques used to evaluate the morphological changes induced by laser annealing in their specific study [8]. The nano Boron surface temperature after laser shot given by [9-11]

$$T_{(0,t<\tau)} = T0 + \frac{2I_0(1-R)(Nt)^{\frac{1}{2}}}{K} \quad (1)$$

where T_o initial surface temperature (29K), I: R: reflectivity 0.74 at 1.064 μm, K: thermal conductivity W/cm. k), N: thermal diffusivity (cm^2/s), and t: pulse duration (7ns). The thermal properties were measured by transient (frequency-domain) 3ω method (FDTR technique) by depositing cooper micro heater/sensor design as in figure (3, a).

1 Samples and Experimental Details

The crystalline wafer of p-type silicon with a resistivity of 3.5 Ω.cm, 508 μm thickness, and (111) orientation was used as starting substrates. The substrates were cut into a square with areas of 1×1 cm^2. The native oxide was cleaned in a mixture of HF and H_2O (1:2). After chemical treatment, Photo-electrochemical etching was performed in a mixture of 48% (1:1) HF-Ethanol at room temperature using a Pt electrode. The schematic diagram of the electrochemical etching system is shown in Fig. 1. The porous area was 1 cm^2, and as-prepared porous silicon was dried by rapid hot air (using a drayer) and stored in a container containing ethanol to reduce oxidization and contaminations. The current of 40 mA/cm^2 was applied for 10 min. Samples were illuminated by a semiconductor green laser 514.5 nm and powered at 100 mW. The rapid thermal oxidation (RTO) system consists of the tungsten halogen lamp type (OSRAM 64575) with a power of 1000 W based on a ceramic base. A parabolic reflector-like half circuit was put under the lamp to increase the heating efficiency. (2) A quartz tube has a 3 cm diameter opening from two sides to circulate the dry oxygen source. The quartz tube is attached to a halogen lamp to obtain the desired temperature. The RTO temperatures are 30 Ċ at an oxidation time of 60 s. They can be calibrated using a thermocouple type J with a digital reader above the sample.

The nano-boron (n-B) was deposited on the $PSiO_2$ surface, and n-Boron (0.3 mg/L) was dissolved in ethanol. Ethanol is a polar solvent that can dissolve nano boron if it is soluble in this solvent. Ethanol is a commonly used solvent in spin coating due to its low evaporation temperature, which makes it easy to evaporate from the substrate after spin coating. Ethanol is also a relatively safe solvent, but it is flammable and should be handled cautiously. After dissolving, the n-B was deposited by the spin coating method, using a rotation per minute of 3000 for 60 seconds. Then, ten drops of n-B were dropped on the surface of the rotated PSiO2. After that, the n-B thin film was dried at 150°C for 10 minutes to remove any volatile components. These processes were repeated ten times to increase the thickness of the n-B thin film.

Nd: YAG laser used in the experimental work at a wavelength of 1.06 μm. This laser is made by DELIXI and used in this work to provide pulse energy ranging from (50-500) mJ in 7ns pulse duration. A spot diameter focuses the laser beam on the target. In this work, the laser beam diameter on carbon targets is 0.08 cm. The distance between the sample and the laser is 12 cm. The LSP set up a flow chart as in Figure 2.

.

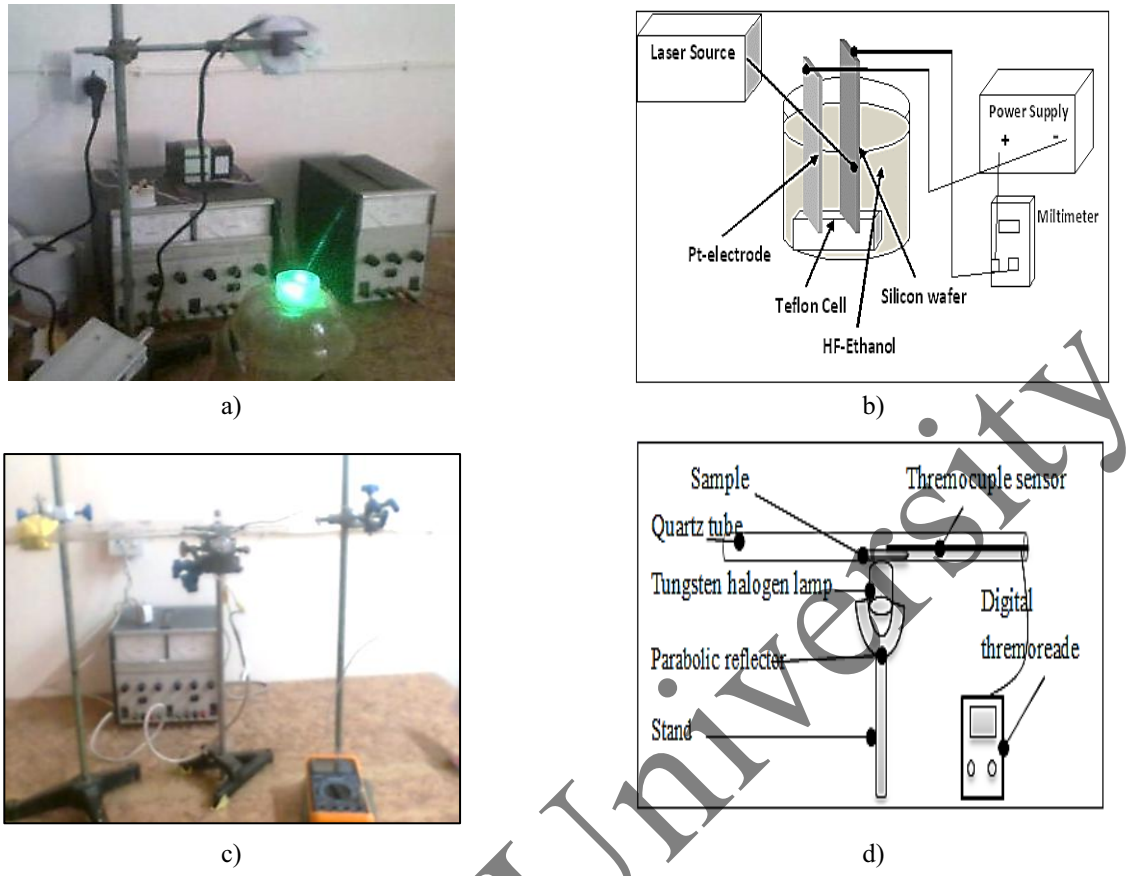

a) b)

c) d)

Fig.1. (a) The schematic diagram depicts the PEC process. (b) The photographic image, (c) The photographic image RTO system, (d) Schematic diagram of the RTO system.

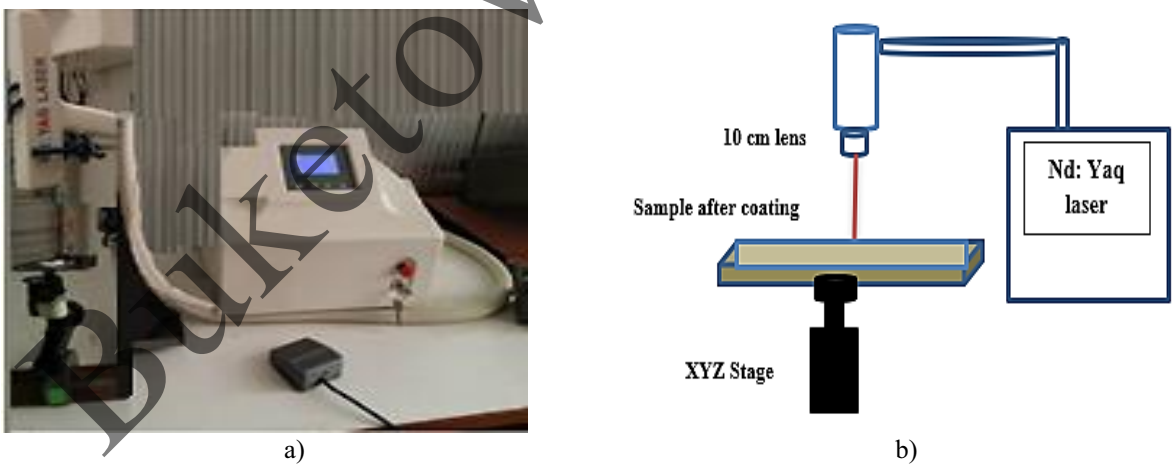

a) b)

Fig.2. Laser annealing images: a) photographic image; b) Schematic diagram

Thermal properties were measured by copper deposited by the evaporation method as a heat sink, shown in Figure 3; the purpose of this measurement is to find the thermal constant used in equation 1 for a calculated surface temperature where thermal conductivity is (113.12 10^{-7} W/cm. k), and thermal diffusivity is (0.27cm^2/s). 0.1 μm-thick silver layers were deposited by one drop on the wafer

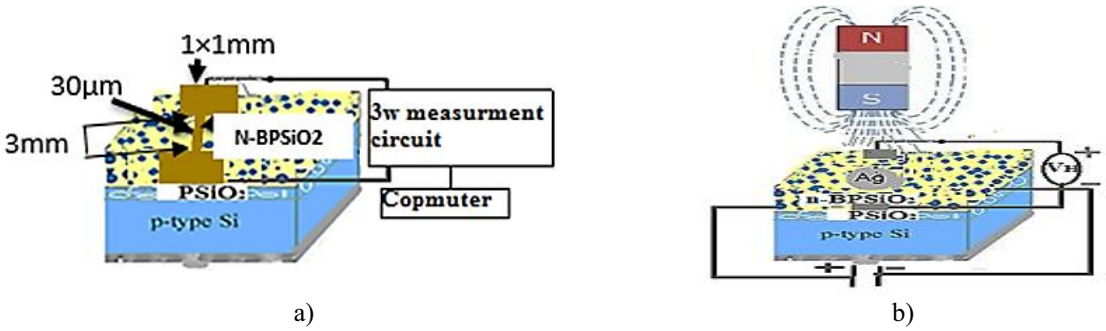

a) b)

Fig. 3. (a) Chart diagram of the experimental 3ω measurement. Finally, n-B thin films were annealed at different overlapping 50:50 by Nd: YAG laser energy and study the prober energy gives the best electrical properties, (b) Hall measurement schematic diagram.

The structure properties, such as surface morphology, layer thickness, and pore diameter, were measured. AFM measured these grain size distributions and surface topography. The silver past electric contacts. Where deposited paste using one drop on samples by Aluminum mask has a circular area of about 3mm^2 and connected wire; after three days, the Aluminum mask was removed, and remain the silver with the connected wire dried; the electric circuit is shown in the figure below as a schematic diagram. The Hall Effect measurement system ECOPIA (HMS-300 VER3.5) input data temperature 300K, current (0.1mA) delay time (0.1s) applied magnetics 0.55T.

2 Results and discussion

2.1 Surface heating temperature

The surface heating temperature was determined from relation (1). Fig.4 (a, b) shows the experimental data of silicon; a photometer from PIER-ELECTRONIC measured the transmission and reflection. At 1064 μm wavelength, the transmission and reflection values were 14% and 74%, respectively; the obtained reflectivity was used to calculate surface temperature. Figure (4, c) shows that the absorption of laser energy can cause increased surface temperature by increased laser energy on the material surface. The laser energy is absorbed by the n-B/$PSiO_2$, which raises its temperature. The magnitude of the temperature increase depends on various factors, such as the absorption coefficient of the material, the laser fluency, and the duration of the laser exposure. In addition, the material's thermal conductivity also plays an essential role in the magnitude of the temperature increase. Materials with low thermal conductivity will have higher temperatures, as heat is not efficiently transferred away from the surface. It's essential to consider the effects of the increased temperature on the material, as it can cause structural changes, chemical reactions, and other effects that can impact the material's properties [10 -12].

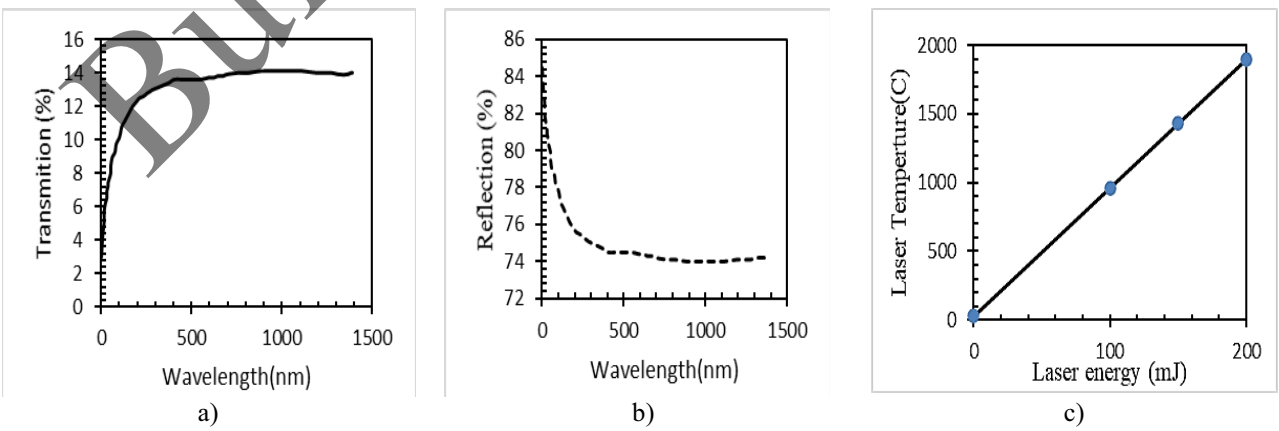

a) b) c)

Fig.4. The (a) transmission and (b) reflection measurement of n-B deposited on OPSi, and (c) Laser temperature on the surface at different laser energies.

2.2 Atomic Force Microscopy

Atomic Force Microscopy (AFM) analysis is a powerful tool for investigating materials' surface morphology and roughness, including nano-sized boron deposited on oxide porous silicon before and after annealing it by laser. An AFM obtained high-resolution images of the surface at the nanoscale. It obtained information about the surface topography, roughness, and any parameter changes due to annealing with different laser energies. Fig.5. Show the AFM images before and after annealing samples with different laser energies, which cause changes in the surface morphology and roughness of the material.

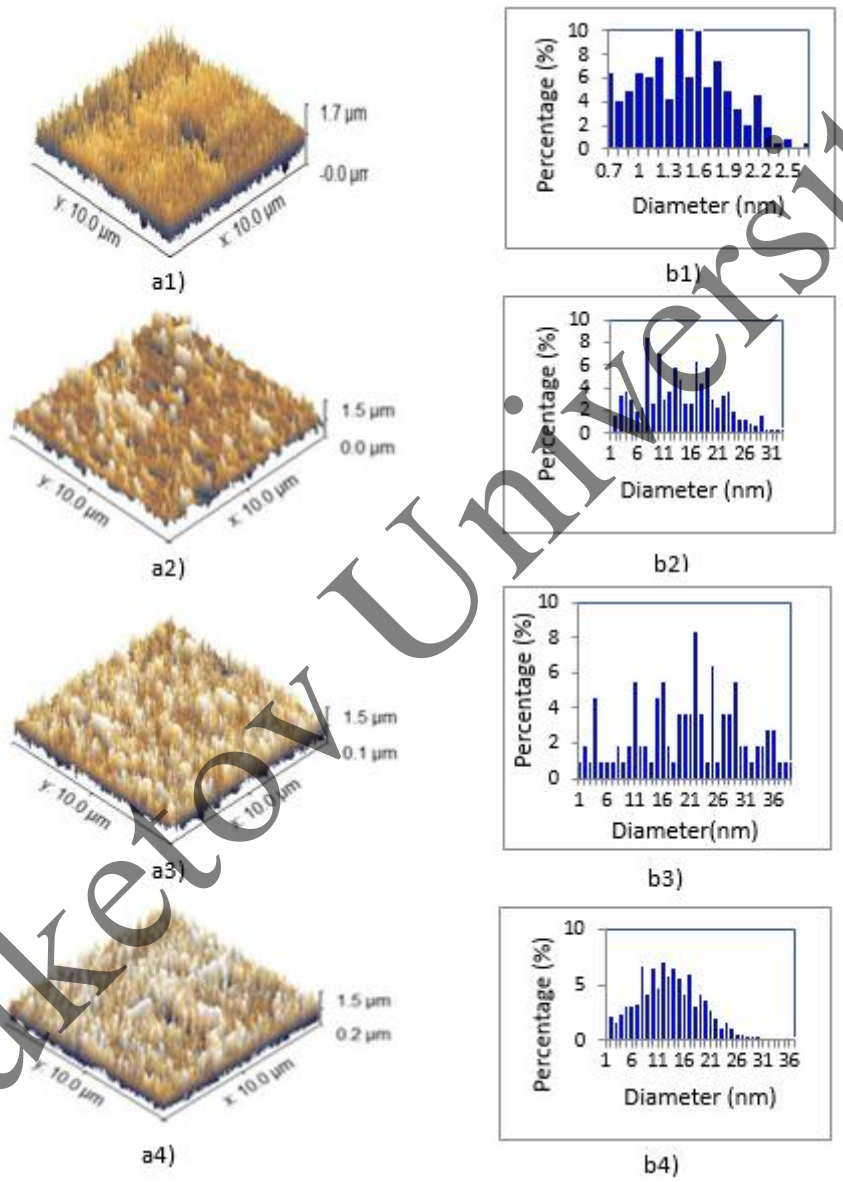

Fig.5. AFM images (a1) before laser annealing, (a2) 100mJ, (a3) 150mJ, and (a4) 200mJ laser energy, while (b1, b2, b3, and b4) represented grain size distribution.

The number of grains increased by increased laser energies after annealing being influenced by various factors, including the laser energy used during the annealing process. In the case of nano boron deposited on oxide porous silicon, increasing the laser energy can increase the number of grains. Higher laser energy can cause a higher temperature during the annealing process, leading to more rapid and intense n-B/PSiO$_2$ recrystallization, new grains' formation, and the growth of existing grains, increasing the number of grains [13]. Additionally, the increased laser energy can promote boron diffusion and segregation within the material, further promoting grain growth and the formation of new grains. The laser energy 100mJ generated

a heat temperature of 963C, causing structural defects in the material to anneal and heal, leading to a more ordered and uniform grain structure; increasing laser energy decreased the maximum grain size [14].

When annealing of n-B/$PSiO_2$ at laser temperatures of 1430°C and 1897°C. The results show that the maximum grain size of the material decreased after the annealing process. The decrease in grain size can be attributed to several factors, such as the increased concentrations of the material's atomic structure at high temperatures, which can lead to grain boundary migration and the formation of smaller grains. The n-B may also influence the grain growth behavior of the $PSiO_2$ material. It is important to note that a material's grain size and structure can significantly impact its physical and mechanical properties. Understanding how to control the grain size through processes such as annealing is vital in developing advanced materials. [15, 16]

Surface roughness refers to the small-scale deviations of a surface from its average height. At the annealing temperature of 963°C, the surface roughness of the n-B/$PSiO_2$ decreased after the annealing process. For example, the decrease in surface roughness after annealing laser energy 100 mJ due to several factors; I. The migration of grain boundaries can lead to a more homogeneous and smooth grain structure; II. Although the recrystallization of the material can result in the formation of larger and more uniform grains, the surface roughness of the n-B/$PSiO_2$ increased after annealing by laser energy 150 and 200mJ that heated the surface temperatures to 1430°C and 1897°C respectively, due to several factors, such as the formation of new grain boundaries, which can lead to a more heterogeneous grain structure. In addition, the precipitation of secondary phases can result in the formation of tiny, localized rough features on the surface [17]; the grain size information and surface properties are shown in Table 1.

Table 1. The grain and surface information estimated from AFM analysis for annealing n-B/$PSiO_2$, (a) without laser annealing, (b) 100mJ, (c) 150mJ, and (d) 200mJ laser energies.

Sample no.	Total grain number	Avg. diameter (nm)	Maximum grain high(nm)	Surface roughness (nm) Rq	Surface area ratio $\times 10^4$
a	320	1.41	1.4	19.3	15
b	293	1.94	2.3	15.1	6
c	887	1.86	1.8	20	16
d	1227	1.51	1.4	20	21

2.3 Electrical and Magnetic Properties

2.3.1 I-V Characteristics

Both forward and reverse currents were increased after annealing by Nd: Yag laser with different energies. Figure 6 shows that increased current before annealing nano boron deposited on porous oxide silicon because of oxygen-related defects in the n-B/$PSiO_2$ can impact the charge transport and increase the forward and reverse currents [17]. The decrease in forward and reverse current after annealing is due to many reasons.

I. Surface morphology: The laser annealing process can alter the surface morphology of the nano boron deposited on the porous oxide silicon, decreasing the forward and reverse currents due to the nano boron particles fusing or aggregate, creating areas of high resistance that can impact charge transport [18].

II. Laser annealing can alter the interface states between the nano boron and oxide porous silicon and decrease forward and reverse currents. The formation of new interface states can increase the interface's resistance and impact the material's charge transport [19];

III. Dopant activation: laser annealing can help to activate the dopants in the nano boron, leading to improved charge transport and reduced forward and reverse current [20];

IV. Oxygen Content: The annealing process can also lead to the formation of oxygen-related defects in the n-B/$PSiO_2$, which can impact the charge transport and increase the forward and reverse currents [21].

.

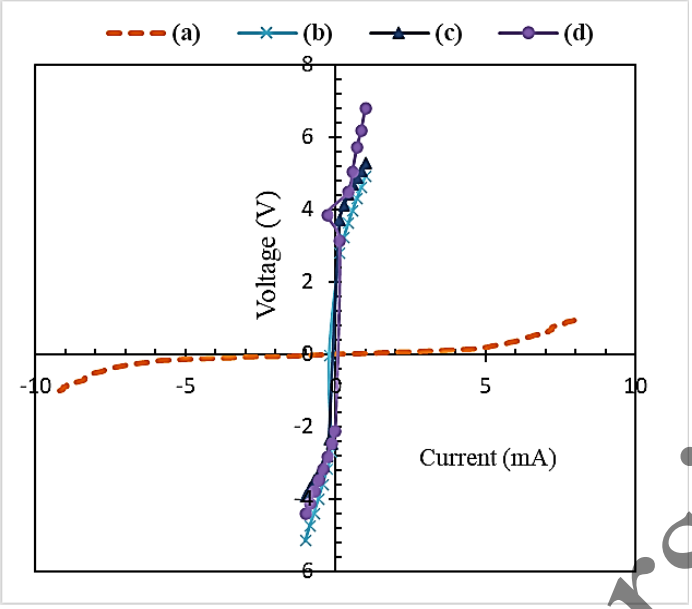

Fig.6. I-V characteristics of n-B/PSiO$_2$ (a) before laser annealing, (b) 100mJ, (c) 150mJ, and (d) 200mJ laser energy.

2.3.2 Electrical and Magnetic Parameters

The occurred electrical parameters like; electrical resistivity, Electron mobility, bulk concentration, and hall constant are shown in Figure 7. In the Fig. (7, a), the electrical resistivity is increased with increased laser annealing temperature, which can be attributed to several factors; Firstly, introducing high-energy laser radiation to the n-B/PSiO$_2$ material can cause defects in the crystal lattice structure of the material. These defects can act as scattering centers for the electrons in the material, leading to increased electrical resistivity [22]. Secondly, high-energy laser radiation can cause an increase in the concentration of impurities or dopants in the n-B/PSiO$_2$ material, which can also contribute to an increase in electrical resistivity because impurities or dopants can introduce additional energy levels in the band gap of the material, which can trap electrons and increase resistivity. Finally, high-energy laser radiation can cause thermal effects in the n-B/PSiO$_2$ material, such as localized heating or melting, altering its electronic properties and increasing resistivity [23].

Fig. (7, b) shows that the decrease in electric mobility with increasing laser annealing energy of nB deposited on OPS is due to several factors. One of the primary factors is the formation of defects in the material. The high energy of the laser beam can disrupt the crystal lattice structure of both the nB and OPS, leading to the formation of defects that act as traps for electrons. These defects can decrease the electrons' mobility and reduce the material's overall conductivity. The thermal annealing effect is another factor that can contribute to the decrease in electric mobility. When the material is subjected to high temperatures during laser annealing, there can be a reduction in the number of charge carriers, such as electrons, due to the formation of thermally activated defects, leading to a decrease in electric mobility. Overall, the decrease in electric mobility with increasing laser annealing energy of nB deposited on OPS results from the formation of defects and thermal annealing effects [21]. The authors [24] suggest the possibility of varying the change in the concentration of defects and impurities. The Defects in vacancies, interstitials, or impurities can arise during fabrication or through the interaction between boron and the underlying silicon oxide layer. Some possible defects in this system include; Boron Vacancies: Vacancies occur when boron atoms are missing from their lattice positions.

These vacancies can act as scattering centers for charge carriers and influence electrical conductivity; Silicon Vacancies: Similarly, vacancies in the silicon lattice can be introduced during the fabrication process or due to the interaction with boron. Silicon vacancies can also affect the electronic properties and conductivity of the material; Interstitials: Interstitials are atoms or ions that occupy positions between the regular lattice sites. Interstitial boron or silicon atoms can disrupt the crystal structure and influence conductivity [25]; Surface Defects: The presence of defects at the surface, such as dangling bonds or surface

states, can affect the electronic properties and charge transport at the interface between the n-B and $PSiO_2$ layers [23]; Regarding impurities, they can be introduced during the deposition process or originate from the starting materials. Some impurity mechanisms relevant in this system include; Contaminants in the Boron source: Impurities can be unintentionally introduced if the boron source used during the deposition process contains impurities. These impurities could be elements or compounds not desired in the final material; Diffusion from the substrate: The oxidized porous silicon ($PSiO_2$) substrate can release impurities through diffusion processes during the annealing step. These impurities could originate from the silicon oxide layer or underlying silicon substrate [26]; Gas contamination: If the deposition or annealing processes occur in an environment with impure gases, such as residual oxygen, moisture, or other contaminants, they can contribute to the formation of impurities in the n-B thin films

Fig. (7, c) shows increased bulk concentration with increasing laser annealing energy of n-B/$PSiO_2$ because the oxide on porous silicon enhances its surface area and reactivity [23]. When the laser energy is increased, it can lead to higher temperatures and more intense heating of the nano boron and porous silicon substrate resulting in various effects, such as improved crystallization of the boron and enhanced diffusion of the boron atoms into the substrate. As a result, the bulk concentration of the nano boron can increase with increasing laser annealing energy can benefit various applications, such as developing advanced electronic and optoelectronic devices. However, optimizing the laser annealing conditions is essential to achieve desired properties without causing damage or degradation to the materials.

In Fig. (7, d), The Hall coefficient is a material property that describes the behavior of charge carriers in a magnetic field and is defined as the ratio of the electric field to the product of the magnetic field and the current density. The sign of the Hall coefficient determines the type of charge carriers (electrons or holes), and the magnitude of the coefficient depends on their concentration and mobility [27]. In the case of n-B/$PSiO_2$, the laser annealing process can affect the Hall coefficient; when n-B/$PSiO_2$ is subjected to laser annealing, the Hall coefficient can show an interesting behavior with changes in laser annealing temperature. Specifically, the Hall coefficient may increase with laser annealing temperature up to a certain point of 963 Ċ due to enhanced diffusion of nano boron atoms into the substrate, increasing the carrier concentration. Decreasing with a further increase in laser annealing temperature. When the laser energy is increased, it can lead to higher temperatures and more intense heating of the n-B/$PSiO_2$, which can result in various effects, such as improved crystallization of the boron and enhanced diffusion of the boron atoms back out of the substrate, resulting in a decrease in the carrier concentration and a corresponding decrease in the Hall coefficient. Therefore, the Hall coefficient of nano boron deposited on silicon can exhibit a non-monotonic behavior with changes in laser annealing temperature, increasing to a specific temperature before decreasing with further temperature increases. This behavior can be necessary to consider when optimizing the laser annealing conditions for the desired electrical properties of the material. The nano boron is represented as a paramagnetic metal inversely proportional to applied annealing laser energy that decreases the hall coefficient; some reports talk about decreased boron magnetism susceptibility (χ_{par}) with increasing temperature [10].

Figure (7, e) shows that increased magnetoresistance with increasing laser temperature is attributed to the tunnel injection through the thin silicon dioxide layer causing a charge acceleration and providing the energy to trigger a transition to a high mobility transport regime by an autocatalytic impact ionization process [27]. A small annealing laser temperature probably causes shrinkage of the acceptor wave functions, and the overlap by the tails is reduced for an average pair of neighboring acceptors. The effective acceptor energy level increases concerning the valence band, by which the activation energy for impact ionization significantly increases, strongly suppressing the current. The quasi-neutrality breaking of the space-charge effect causes insufficient charge to compensate for the electrons injected into the device. They speculate that in the regime of electric field inhomogeneity, the motion of electrons becomes correlated and thus dependent on applying laser energy or being a component to construct spin logic [28]. The relationship between magnetoresistance and sheet concentration is shown in Figure (7, f). An increase in sheet concentration can lead to an increase in magnetoresistance because increasing the concentration of magnetic particles or impurities in a material lead to a more robust response to an applied magnetic field, resulting in a more significant change in resistance, also annealing n-B/$PSiO_2$ may be changed the electronic properties due to the structure of the material changes, or changes in the interaction between the material and the magnetic field [29, 30].

In the context of the relationship between the change in the concentration of defects and impurities and the change in electrical conductivity, when considering a charge transfer mechanism as ballistic, the charge

.

carriers (electrons or holes) move through the material without scattering or colliding with impurities or defects. In this idealized scenario, the charge carriers' concentration and mobility determine the material's electrical conductivity [31]. In the case of n-B/PSiO$_2$, the concentration of defects can have a twofold effect on the change in the conductive properties.

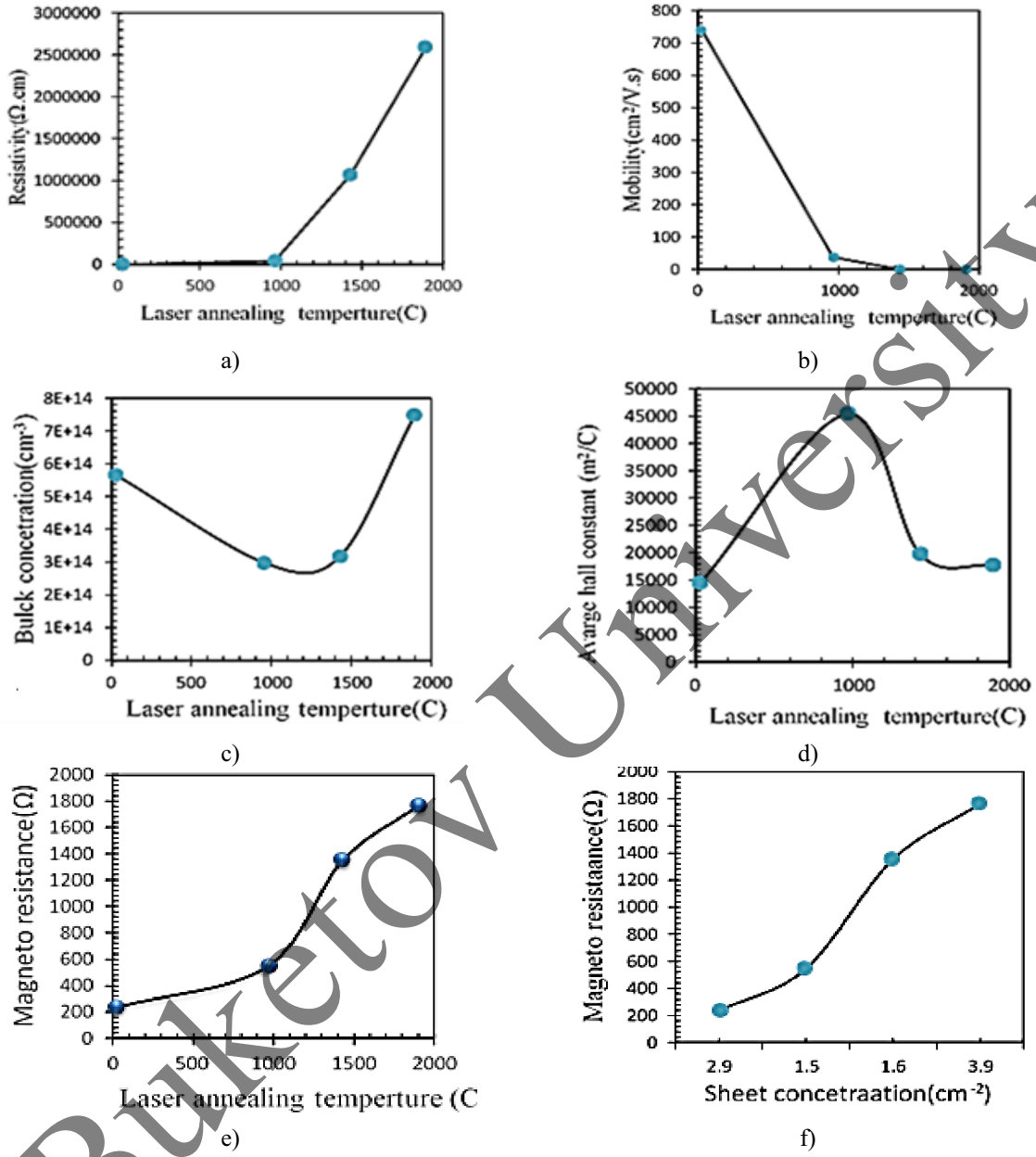

Fig.7. Electrical parameters of n-B/PSiO2 before and after annealing at different laser energy with (a) resistivity, b) mobility, (c) bulk concentration, (d) average Hall constant, (e) Magneto resistance Vis different laser annealing, (f) Magneto resistance Vis material sheet concentrations.

Let's break it down; Defects as scattering centers: Defects such as vacancies, interstitials, or impurities can act as scattering centers for charge carriers. When charge carriers encounter these defects, they experience scattering, reducing their mobility and decreasing electrical conductivity [32]. Higher defect concentrations would result in increased scattering, leading to a more significant decrease in conductivity; Defects as dopants: Impurities or defects can also act as dopants, introducing additional charge carriers into the material. Depending on the nature of the defects and their energy levels relative to the material's band structure, they can either contribute to the population of charge carriers (n-type doping) or create electron-hole pairs (p-type doping). This additional population of charge carriers increases the overall electrical

conductivity of the material. Therefore, higher defect concentrations can lead to a higher concentration of dopants, resulting in increased conductivity [33].

Now, when n-B thin films are annealed using an Nd: YAG laser at varying energies, the annealing process can affect the concentration and distribution of defects in the material. The laser energy can modify the arrangement of boron atoms and their interactions with the surrounding silicon and oxygen atoms, leading to changes in defect concentration. If the laser annealing process reduces the concentration of defects, it would likely result in improved crystallinity and reduced scattering of charge carriers, leading to an increase in electrical conductivity. Conversely, if the annealing process introduces additional defects or disturbs the existing defect structure, it could increase scattering and decrease electrical conductivity [34].

In the case of n-B/PSiO_2 and considering a ballistic charge transfer mechanism, the concentration of defects can influence the electrical conductivity through two mechanisms: scattering of charge carriers and introducing additional charge carriers as dopants. The annealing process using an Nd: YAG laser at varying energies can alter the defect concentration, thereby affecting the conductive properties of the n-B thin films.

The relation between the Hall coefficient and magnetoresistance is shown in Figure 8, where the average Hall coefficient increased at 545 Ω magnetoresistance and decreased at 1352 and 1764 Ω. The Hall coefficient is a material property related to the behavior of charge carriers in a magnetic field.

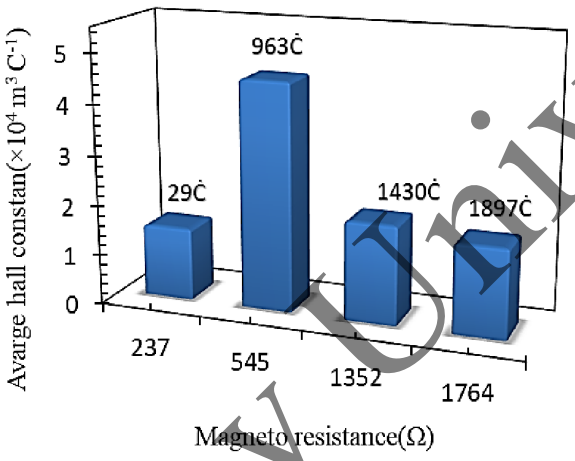

Fig. 8. Magneto resistance Vis average hall constant

When the hall coefficient increases, the material's charge carrier concentration or mobility increases in the presence of a magnetic field. Hence, n-B/PSiO_2 at an annealing temperature of 963 C generates a stronger electric field for a given magnetic field. While decreased hall coefficient at magnetoresistance 1352 and 1764 Ω suggests that the n-B/PSiO_2 is generating a weaker electric field for a given magnetic field, which could be due to a decrease in the number of charge carriers, a decrease in their mobility, or a combination of both. In general, the decrease in nano boron magnetism susceptibility (χ_{par}) with the increasing annealing temperature changes in the Hall coefficient can be used to infer information about the charge carriers in a material, such as their density and mobility. It is a helpful tool for the electronic properties studying of materials during magnetoresistance [35,36].

Conclusions

This study concludes that laser annealing is an essential technique for tailoring the electrical properties of n-B/PSiO_2. Still, the optimization of laser annealing conditions is essential to achieve the desired properties without causing damage or degradation to the material. The study found that laser annealing with different energies can affect surface morphology, electrical resistivity, electric mobility, bulk concentration, Hall coefficient, and magnetoresistance of n-B/PSiO_2. Increasing laser annealing energy can improve the material's electrical conductivity, increase surface roughness, and introduce defects and impurities. The non-monotonic behavior of the Hall coefficient with changes in laser annealing temperature is an important consideration when optimizing the laser annealing conditions for the desired electrical properties of the material. The study provides valuable insights into the impact of laser annealing on the properties of n-

$B/PSiO_2$ and can inform the development of new materials and applications; the increased electrical resistivity of n-B/OPSi with increasing laser annealing energy due to many factors, including the introduction of defects, an increase in impurity or dopant concentration, and thermal effects. Increasing the laser annealing temperature can generally lead to changes in the crystal structure, defect density, and carrier concentration, affecting the Hall coefficient. As I mentioned earlier, the Hall coefficient measures the electric field ratio to the magnetic field in a material. Therefore, a decrease in the Hall coefficient suggests that the material generates a weaker electric field for a given magnetic field. This could be due to a decrease in the number of charge carriers, their mobility, or a combination of both.

In summary, the increase in the number of grains observed with increasing laser energy of nano boron deposited on porous oxide silicon can be attributed to the influence of laser energy on the recrystallization and grain growth processes in the material. The grain size reduction, in this case, may result in improved mechanical, electrical, or thermal properties of the material. The application prospects strongly motivate this research and show huge magnetoresistances in $n\text{-}B/PSiO_2$ after Nd: YAG laser annealing at energy 200mJ. The device could be suitable as a magneto-resistive sensor for high-density data storage, forming the basis of an avalanche spin-valve transistor. Furthermore, this behavior can be necessary to consider when optimizing the laser annealing conditions for the desired electrical properties of the material.

Acknowledgments

In this paper, we would like to thank the people who assisted in completing this work.

REFERENCES

1 Seliverstova E.V., Ibrayev N. Kh., Alikhaidarova E.Zh. The Effect of Laser Energy Density on the Properties of Graphene Dots. *Eurasian Physical Technical Journal*, 2022, 19, No.2 (40), pp.30-34.

2 Chen A.A review of emerging non-volatile memory (NVM) technologies and applications. *Solid-State Electronics,* 2016, 125, pp.25-38.

3 Sun J., Kosel J. Extraordinary Magnetoresistance in Semiconductor. Metal Hybrids: A Review. *Materials*, 2013, 6, pp. 500-516.

4 Porter N., Marrows C. Linear magnetoresistance in n-type silicon due to doping density fluctuations. *Scientific Reports*. 2012, 2, 565 p.

5 Narjis Z. Non-Distractive Testing by Nanosecond Nd: Yag Laser Technique as Alternative Method to Find Nano -ZnO/Al Properties. *Laser manufacturing and material processing*. Accepted. 2023. doi:10.21203/rs.3.rs-2625199/v1

6 Alwan M.A. , Abdalzahra N.Z. The influence of heating treatment on physical properties of porous silicon. *Al-Nahrain Journal of Science*, 2009, 12, 2, pp.76-81.

7 Mahbubur M.R., et. al. Effects of annealing temperatures on the morphological, mechanical, surface chemical bonding, and solar selectivity properties of sputtered TiAlSiN. *Thin films. Journal of Alloys and Compounds,* 2016, 671, pp. 254-266.

8 Zamil N. Ultrasonic shock wave generated by laser as an alternative method to find different bone properties. *Lasers in Medical Science,* 2023, 38:138, pp.1-15.

9 Theerthagiri J., Karuppasamy K., Lee S.J., et al. Fundamentals and comprehensive insights on pulsed laser synthesis of advanced materials for diverse photo- and electrocatalytic applications. *Light: Science & Applications*, 2022, 11, 250 p.

10 Zamil N. Ultrasonic shock wave generated by laser as an alternative method to find different bone properties. *Lasers in Medical Science,* 2023, 38:138, pp.1-15.

11 Sands D. Pulsed laser heating and melting, heat transfer. *Engineering Applications,* 2011, pp. 47-70.

12 Zamil N. Assessment of Surface Modification by Laser Studies of Polymer Material before and after M.B. Doping. *New Trends in Physical Science Research*, 2022, 1, pp. 123-132.

13 Chaurasia S., *et al*. *Simultaneous measurement of particle velocity and shock velocity for megabar laser-driven shock studies*. *Barc Newsletter*, 2010, 317 p.

14 Colvin J., Larsen J. Extreme Physics Properties and Behavior of Matter at Extreme Conditions. *Cambridge University Press,* 2013.

15 Zamil N. Laser–Driven Acoustic Waves: Physical Properties of Paramagnetic Metal. Research & Reviews. *Journal of Pure and Applied Physics*, 2022, 10, 6, pp.1-6.

16 Khudhair W.A., Zamil N. Laser Nanosecond Technique, FTIR and AFM Application to Find Physical Properties of PVA Doped with Dye. *New Trends in Physical Science Research*, 2022, Vol. 7, pp.73-85.

17 Cristiano F., La Magna A. Laser Annealing Processes in Semiconductor Technology Theory, Modeling, and Applications in Nanoelectronics, *A volume in Woodhead Publishing Series in Electronic and Optical Materials*, 2021, 200, 210p.

18 Wang Y., *et al*. Laser spike annealing and its application to leading-edge logic devices. *Conference: Advanced Thermal Processing of Semiconductors. 16th IEEE International Conference* (2008).

19 Liu X., *et al.* Aggregation and deposition behavior of boron nanoparticles in porous media. *Journal of Colloid and Interface Science,* 2009, 330, 1, pp. 90-96.

20 Zizi A., *et al*. The effect of ND-YAG laser surface treatment on mechanical properties of carburizing steel AISI 1006. *Journal of Engineering Science and Technology*, 2020, 15, 6, pp. 3891 - 3902.

21 Hamoudi W.K., Raouf D.N., Zamil N. Laser-Induced Shock Wave Studies of Para and Ferro Magnetic Materials. *J Material Sci Eng*., 2017, 6, 3, pp. 1000349.

22 Alwan M.A., Narges Z.A., Halim N.H.A. Influence of rapid thermal oxidation process on the optoelectronic characteristics of PSI devices. *Int. J. Nanoelectronics and Materials*, 2009, 2, pp. 157 – 161.

23 Zamil N. Porous Silicon on Insulator Technology. *Journal of Scientific Research and Reports.* 2022, 28, 1, pp. 98-106.

24 Zamil N. The Structure and Electrical Properties of Porous Silicon Prepared by Electrochemical Etching. *Iraqi Journal of Physics*, 2011, 9, 15, pp. 94-101.

25 Zamil N. Electrical Properties of Oxidized Porous Silicon. *Al- Mustansiriya J. Sci*., 2009, 20, 4, pp. 59-68.

26 Paul A., Laurila T., Divinski S. Handbook of Solid State Diffusion. *Diffusion Fundamentals and Techniques,* 2017, Vol. 1, pp. 1-54.

27 Zamil N. The Effect of Laser Wavelength on Porous Silicon formation mechanism, *NUCEJ.* 2011, 14, pp.197-101.

28 Alberi K., Scarpulla M.A. Suppression of compensating native defect formation during semiconductor processing via excess carriers. *Scientific Reports*, 2016,6, 27954.

29 Zeena M.A., Narges Z., Hammood I.H. Optical Properties of Tap Water Purity using He-Ne Laser with Different Power Density. *Al-Nahrain Journal of Science*, 2014, 17, 3, pp.99-107.

30 Schoonus J., *et al*. Unraveling the mechanism of sizeable room-temperature magnetoresistance in silicon. *J. Phys. D: Appl. Phys*., 2009, 42, 185011.

31 Nicholas A., *et al*. Linear magnetoresistance in n-type silicon due to doping density fluctuations. *Scientific Reports*, 2012, 2, 565p.

32 Silva A., *et al*. Magnetoresistance of doped silicon", *Physical Review B.*, 2015, 91, pp. 214414.

33 Zhao Y., Tripathi M., et al. Electrical spectroscopy of defect states and their hybridization in monolayer MoS_2. *Nature Communications*, 2023, 14, pp. 44.

34 Komsa H.P., Krasheninnikov A.V. Defects in Two-Dimensional Materials. Chapter 2 - Physics and theory of defects in 2D materials: the role of reduced dimensionality. *Materials Today,* 2022, pp. 7 – 41.

35 Alwan M.A., Khalaf W.K., Abdulzahra N.Z. Physical Properties of MOS Porous Silicon Detector Fabricated under RTO Method. *Eng. & Tech. Journal,* 2009, 27, 11, pp. 2286 – 2290.

36 Gupta M., et al. *Handbook of Laser Micro- and Nano-Engineering*, 2020, 31 p.

37 Saraswati V., Paulose P. Magnetic susceptibility and magnetic resonance in boron and boron carbides. *Journal of the Less Common Metals*, 1987, 128, pp. 185-193.

Article accepted for publication 01.05.2023